The Journal of Experimental Biology 213, 426-432

doi:10.1242/jeb.033563

Limits to vertical force and power production in bumblebees (Hymenoptera: *Bombus impatiens*)

R. Buchwald[1,*] and R. Dudley[1,2]

[1]Department of Integrative Biology, University of California, Berkeley, Berkeley, CA 94720 USA and [2]Smithsonian Tropical Research Institute, Balboa, Republic of Panama

*Author for correspondence (rbuchwald@gmail.com)

Accepted 21 October 2009

SUMMARY

Maximum vertical forces produced by flying animals can be difficult to identify unequivocally, but potentially indicate general limits to aerodynamic force and muscle power output. We used two methods (i.e. incremental addition of supplemental mass and asymptotic load lifting) to determine both the intraspecific allometry of and methodological differences in estimates of maximum flight performance for the bumblebee *Bombus impatiens*. We found that incremental mass addition underestimated maximum lifting capacity by approximately 18% relative to values obtained by asymptotically increasing the applied load during a lifting bout. In asymptotic loading, bumblebees lifted on average 53% of their body weight, and demonstrated a significantly negative allometry of maximum aerodynamic force production relative to thoracic muscle mass. Estimates of maximum body mass-specific mechanical power output increased intraspecifically with body mass to the 0.38–0.50 power, depending on values assumed for the profile drag coefficient. We also found a significant reduction in vertical force production when both hindwings were removed. Limits to load-lifting capacity ultimately co-occur with an upper bound on stroke amplitude (~145 deg.). Although thoracic muscle mass showed positive allometry, overall load-lifting performance exhibited significant size-dependent degradation.

Supplementary material available online at http://jeb.biologists.org/cgi/content/full/213/3/426/DC1

Key words: allometry, *Bombus*, bumblebee, flight, hindwing, hovering, power.

INTRODUCTION

The whole-body forces produced by volant animals potentially influence diverse features of flight biology, including the ability to avoid predators, to chase mates and evade suitors, and to carry nutritional resources. Data on extreme features of axial agility (i.e. maximum translational accelerations along the three orthogonal body axes) are, however, difficult to obtain given uncertainty in differentiating between behavioral propensity and physiological capacity to perform at maximum levels. Body size exerts a strong influence on flight performance, but allometric studies of both intraspecific and interspecific variation in flight performance have yielded inconsistent results. In an important study, Marden attached lead weights cumulatively to the legs or abdomens of numerous species of birds, bats and insects until the animals were unable to take off from the ground (Marden, 1987). The capacity for maximum vertical force production was approximated from the average weight lifted immediately prior to and subsequent to unsuccessful takeoff. Marden concluded that vertical force production scaled isometrically with thoracic muscle mass across species (Marden, 1987). Subsequent power estimates using the same data set (Marden, 1990) derived a positive interspecific allometry for total mechanical power (but see Ellington, 1991).

More recently, an asymptotic load-lifting method has been applied to both hummingbirds and orchid bees to evaluate maximum vertical force production (Chai et al., 1997; Altshuler and Dudley, 2003; Dillon and Dudley, 2004). By attaching a beaded string near the center of body mass of the animal and then eliciting vertical escape, more and more weight is lifted off the ground until the animal transiently hovers in the air while sustaining maximum load; this limit is approached asymptotically as the lifted mass increases at a decreasing rate and the animal progressively slows. This method avoids potential complications of fatigue, as the animal attains maximum lifting capacity in a single vertical bout. Asymptotically applied loads also enable the animal to rise substantially above the resting position, avoiding both transient takeoff effects and the ground effect (see Dudley, 2000). Among 11 species of orchid bees, maximum lifted loads varied isometrically with body mass but exhibited a negative allometry relative to thoracic muscle mass, in contrast to the interspecific allometry obtained by Marden (Marden, 1987). Neither study, however, incorporated phylogenetic relatedness of study taxa, which may be a confounding effect when comparing insects with volant vertebrates. Here, we investigated load-lifting abilities in the bumblebee *Bombus impatiens*, the adult workers of which exhibit a nearly four-fold range in body mass, to determine associated intraspecific allometries in maximum vertical force and power production, and to compare results of the two aforementioned experimental methods.

Reductions in wing surface *via* abrasion and predator-induced damage may have important consequences for flying animals. Wing degradation in bumblebees typically involves losses from the trailing edge, and can reduce overall survivorship (Cartar, 1992). In the bumblebee *Bombus terrestris*, a 10% decrease in wing area effected by distal clipping resulted in compensatory increases in wingbeat frequency, although mechanical power estimates and rates of carbon dioxide production were unchanged (Hedenström et al., 2001). Effects of wing area reduction on maximum flight capacity are unknown in insects, but likely would derive from an absolute increase in wing loading as well as from impairment of the unsteady aerodynamic mechanisms used in flight. For large bees, removal of the mostly basally located hindwings will reduce wing area by ~25%

without influencing the forewing's leading edge and tip regions that serve most prominently in aerodynamic force generation. We accordingly evaluated the effects of hindwing removal on maximum load lifting by bumblebees, using the same unmanipulated individuals as controls.

MATERIALS AND METHODS

Mature colonies of bumblebees (*Bombus impatiens* Cresson) were housed in vented plastic boxes kept within cardboard containers (Koppert Biological Systems, Romulus, MI, USA). Sucrose solution was provided *ad libitum*, and fresh pollen was provided once a week. Colonies were kept at 22°C, and on a 12 h:12 h L:D cycle. Immediately prior to all experiments, the abdomen of test bees was squeezed with soft forceps to empty any nectar stored in the crop. All experiments were conducted at air temperatures from 22 to 24°C with randomly selected adult worker bees.

Loading experiments were carried out using two different methods. In the first approach, which followed closely the protocol described by Marden (Marden, 1987), we progressively attached lead weights averaging approximately 20% of the individual's body mass to the bee's ventral abdominal surface using a small amount of cyanoacrylate. Although the distance of the attached weight from the animal's center of mass may induce a pitching moment on the animal and potentially affect hovering performance, Marden concluded that muscle mass-specific lifting by dragonflies was not affected by the location of the attached weight (Marden, 1987). Once the glue was dry, bees were introduced into a flight arena and induced to fly using ultraviolet illumination from above and then, if necessary, by agitating with forceps. If the insect took off, additional weights were then sequentially added and flight was again repetitively elicited until the animal no longer left the ground. A minimum of five takeoff attempts was used at any given load, with intervening periods of several minutes between successively added weights. The mass of the final load successfully lifted and the mass of the subsequent load not successfully lifted were averaged and added to body mass to approximate the maximum lifted mass (Marden, 1987), which when multiplied by gravitational acceleration yielded an estimate of maximum vertical force ($\mathbf{F}_{vert}$) produced by the insect.

In the second method, we used asymptotic loading as described previously (Chai et al., 1997; Dillon and Dudley, 2004). A beaded string was attached to a bumblebee's petiole such that the first bead group was located 7 cm below the attachment loop, with additional bead groups separated by 2 cm. Although the strings were not attached to the exact center of mass, the petiole is approximately coincident with the center of mass (see Ellington 1984c; Dudley and Ellington, 1990). Bead groups averaged 24.7 mg in mass; the nylon strings had a linear mass density of 0.353 mg cm^{-1}. Following load attachment, we released the bee in a flight chamber similar to that described in Dillon and Dudley (Dillon and Dudley, 2004). An ultraviolet light placed above the chamber stimulated flight. After a short adjustment period when flight was typically erratic, bees began to fly upwards, lifting successive bead groups until no further mass could be lifted and hovering flight was sustained. The first such hovering bout was always discarded, and only bouts greater than 5 cm from the chamber floor were analyzed to avoid ground effects. We tested an individual bee until flight performance visually deteriorated (mean ± 1 s.d.: 11.4±4.2 bouts). The single greatest load lifted during a series of such bouts was used in subsequent analyses given our focus on maximum performance.

A video camera (Sony DCR-TRV19) mounted above the flight chamber filmed both an overhead view and a lateral view of the hovering bee as reflected in a mirror set at 45 deg. to horizontal. An Electret Condenser Microphone (Radio Shack, Fort Worth, TX, USA) was connected to the audio input of the camera and was placed inside the flight chamber to record wingbeat sounds simultaneously on video. Video filming frequency was 60 frames s^{-1} with a shutter speed of 1/250 s. We determined maximum height of the hovering bee from its lateral projection against a coordinate grid on the opposite chamber wall. Maximum load was calculated by first multiplying the linear mass density of the string by the length of lifted string, and then by adding the mass of all beads lifted and the mass of the bee itself. Maximum vertical force ($\mathbf{F}_{vert}$) was then calculated as the product of this total mass and gravitational acceleration.

To evaluate the effects of reduced wing area on maximum load lifting, we first tested individual bees using the asymptotic loading method described above. Both hindwings were then removed at their base using dissecting scissors. The bee was then placed back in the flight chamber with the beaded string still attached, and subsequent lifting bouts were recorded using the aforementioned methods.

For all asymptotic load-lifting trials, recorded video sequences were imported to a computer using Apple iMovie HD and analyzed using NIH ImageJ to determine the horizontal projection of stroke amplitude (Φ_{hor}), based on the maximum and minimum positional angles of the wing (see Ellington, 1984c; Dudley, 1995; Dillon and Dudley, 2004). Stroke plane angles of hovering bumblebees are close to zero (Ellington, 1984a; Dudley and Ellington, 1990), and during maximum load lifting are likely to further decrease [as characterizes orchid bees under aerodynamically challenging hypodense conditions (Dudley, 1995)]. Audio tracks for individual hovering bouts were exported to Raven 1.2.1 (Cornell Lab of Ornithology), and wingbeat frequency (n) was determined from Fourier transforms of acoustic waveforms.

Immediately following experiments with both load-lifting methods, bees were placed in a plastic vial and frozen. Within 4 h, we measured total mass (m), thoracic mass (m_{th}), and the mass of one ipsilateral wing pair. One wing pair, with forewings and hindwings connected in their natural conformation, was then scanned on an Epson 2450 flatbed scanner at 720 d.p.i., and NIH ImageJ was used in conjunction with Microsoft Excel to determine wing length (R), the non-dimensional radius of the second moment of wing area [$\hat{r}_2(S)$], and individual wing area; total wing area (S) refers to the area of both wing pairs and was obtained by doubling the previous measurement. We then calculated aspect ratio AR ($=4R^2/S$) and wing loading p_w ($=mg/S$) for each bumblebee. For a subset of bees, we then cut the thorax in half and placed it in a 0.5 mol l^{-1} NaOH solution for 24 h to dissolve soft tissue. The remaining cuticle was rinsed with water, dried and weighed. Thoracic muscle mass (m_{mus}) was estimated as the difference in mass between the wet thorax and dried cuticle. This method may overestimate thoracic muscle mass, as the NaOH digestion likely dissolved some leg muscles and other structures within the thorax, but the difference will be small as the flight muscles represent nearly the entire volume of bumblebee thoraces (Heinrich, 1970).

Aerodynamic calculations for hovering at maximum load followed Ellington (Ellington, 1984d), and included body mass-specific estimates of induced power, profile power, and total mechanical power assuming perfect elastic energy storage (see Appendix). Spatial and temporal correction factors to the Rankine-Froude momentum estimate of induced power were calculated following Ellington (Ellington, 1984d), and were of the order of 20%. Detailed wingbeat kinematics and empirical measurements of associated unsteady lift and drag (e.g. Sane and Dickinson, 2001)

Table 1. Allometries of morphological and kinematic variables

Parameter	Mean (*N*)	Range	*r*	OLS	95% CL	RMA	95% CL
m_{mus} (mg)	55.6 (37)	31.0–102.5	0.999*	1.21	1.21, 1.22	1.21	1.21, 1.22
R (mm)	10.9 (37)	9.1–13.4	0.930*	0.34	0.29, 0.38	0.36	0.32, 0.41
S (mm^2)	70.3 (37)	49.9–110.1	0.943*	0.68	0.59, 0.76	0.72	0.64, 0.80
$\hat{r}_2(S)$	0.56 (37)	0.53–0.59	–0.1996 (n.s.)	–0.01	–0.04, 0.01	–0.07	–0.05, –0.10
$\hat{r}_3(S)$	0.60 (37)	0.58–0.63	–0.182 (n.s.)	–0.01	–0.03, 0.01	–0.06	–0.04, –0.08
p_w (N m^{-2})	27.2 (37)	21.5–36.6	0.804*	0.32	0.24, 0.41	0.40	0.32, 0.49
AR	6.81 (37)	5.77–8.05	0.0002(n.s.)	-6×10^{-5}	–0.07, 0.07	–0.20	–0.16, –0.30
n (Hz)	181 (29)	155–205	0.755*	–0.20	–0.27, –0.13	–0.27	–0.20, –0.34
Φ_{hor} (deg.)	144 (29)	131–200	0.042 (n.s.)	–0.01	–0.10, 0.08	–0.24	–0.16, –0.34
C_L	2.00 (29)	1.58–2.78	0.041 (n.s.)	–0.02	–0.21, 0.17	–0.46	–0.31, –0.68
Re	2186 (29)	1608–3004	0.866*	0.47	0.36, 0.58	0.54	0.44, 0.65

The data are mean values and sample size (*N*=number of individuals), range, and results of linear regressions on log-transformed body mass of log-transformed morphological and kinematic parameters during maximum cumulative loading, including muscle mass (m_{mus}), wing length (R), wing area (S), non-dimensional radius for the second moment of wing area [$\hat{r}_2(S)$], non-dimensional radius for the third moment of wing area [$\hat{r}_3(S)$], wing loading (p_w), wing aspect ratio (AR), wingbeat frequency (n), horizontally projected stroke amplitude (Φ_{hor}), mean lift coefficient (C_L) and Reynolds number (*Re*).

The correlation coefficient (r) and *P*-values are derived from the hypothesis that there is no correlation between the two parameters. OLS denotes slopes of regression lines calculated by ordinary least squares methods; RMA denotes slopes of regression lines calculated using the reduced major axis method. CL, confidence limit.

*P<0.001; n.s., P>0.05.

would be preferable to time-averaged estimates using the limited set of kinematic data here, but over the limited intraspecific size range under investigation (see Table 1), significant allometric variation in such aerodynamic approximations is unlikely. For estimates of profile power, a profile drag coefficient must be assumed. We followed Roberts and colleagues in using two values for the profile drag coefficient (1.0 and 3.0) to bracket the likely range of values in the absence of detailed angle-of-attack and instantaneous force measurements on flapping bumblebee wings (Roberts et al., 2004). Although aerodynamic force coefficients do exist for revolving insect wing planforms at comparable Reynolds numbers (Usherwood and Ellington, 2002), mean lift coefficients calculated for bumblebees in maximum load lifting substantially exceed the maxima reported for such revolving wings (see Table 1), so that identification of an appropriate profile drag coefficient is precluded using these data. Moreover, no systematic variation with body mass characterized the mean lift coefficient in maximum hovering performance (see Table 1), so that allometric changes in the mean profile drag coefficient are unlikely for the experimental range of bumblebee body masses studied here.

Allometric variation in morphological, kinematic and aerodynamic variables was determined from ordinary least squares (OLS) regressions and reduced major axis (RMA) regressions of log-transformed data. OLS regression was used when one variable was considered to be a predictor of the other variable, and RMA regression was used when both measured variables could be considered dependent. Microsoft Excel 2004 and R 2.6.2 (R Development Core Team), along with a custom-written script for RMA regression (M. Dillon, University of Wyoming) were used for statistical analyses.

RESULTS

We tested a total of 62 *Bombus impatiens* workers. Body mass for this sample averaged 200.1 mg (range: 109–372 mg). For a subset of these bees (N=25), thoracic muscle mass averaged 88.5% of total thoracic mass and 26.1% of body mass. Wing length, wing area and wing loading all scaled isometrically with body mass, whereas thoracic muscle mass demonstrated positive allometry (Table 1).

Body mass-specific maximum vertical force was significantly underestimated in cumulative loading (by about 18% on average) relative to asymptotic load lifting (Table 2). Neither body mass nor thoracic mass differed between the two corresponding sample populations (see Table 2), thereby precluding any size bias. The asymptotic loading method also yielded a significantly negative allometry for maximum vertical force production relative to thoracic muscle mass (Table 3). The slopes of the regression of maximum vertical force on body mass and on thoracic muscle mass were significantly different from the positively allometric regressions derived from cumulative loading data (see Fig. 1), suggesting that the magnitude of underestimation by the second method is size dependent, particularly given the higher accelerations (in this case, during takeoff) that in general characterize smaller animals. Because the cumulative technique derives maximum force production from the average of a successful flight bout and an unsuccessful bout, we could not film bees performing at their maximum with this method. We therefore confined subsequent analysis to results from asymptotic load-lifting alone.

Bumblebees lifted on average about 53% of body weight (range: 11.0–110.0%). When sustaining maximum load in asymptotic lifting, bees hovered for an average duration of 83.3 ms (range: 52.0–298.8 ms), corresponding to approximately 13.6 wing beats

Table 2. Comparison of body mass (m), thoracic mass (m_{th}), and body mass-specific vertical force production ($\mathbf{F}_{vert}/m\mathbf{g}$) in cumulative and asymptotic load-lifting trials

Variable	Cumulative loading (*N*)	Asymptotic loading (*N*)	*t*-statistic	*P*-value
m (mg)	206.5±72.1 (24)	196.0±64.3 (38)	0.598	0.55
m_{th} (mg)	65.3±21.7 (21)	65.6±19.8 (38)	0.058	0.95
$\mathbf{F}_{vert}/m\mathbf{g}$	1.30±0.15 (24)	1.53±0.24 (38)	4.18	<0.0001

Values represent means±s.d. and sample sizes (*N*=number of individuals).

Table 3. Allometric relationships of force and power estimates on morphological and kinematic variables

	$\mathbf{F}_{vert}$			$P_{1.0}$			$P_{3.0}$		
Variable	*r*	OLS	RMA	*r*	OLS	RMA	*r*	OLS	RMA
m	0.880***	0.96	1.09	0.479**	0.18	0.38	0.388*	0.19	0.50
m_{mus}	0.892***	0.79	0.89	0.442**	0.15	0.31	0.334*	0.16	0.41
R	0.823***	2.41	2.93	0.485**	0.52	1.08	0.408*	0.58	1.43
S	0.876***	1.29	1.47	0.566**	0.30	0.53	0.470*	0.33	0.71
p_w	0.647***	1.67	2.58	0.200 (n.s.)	0.18	0.91	0.143 (n.s.)	0.17	1.20
AR	0.164 (n.s.)	–0.79	–4.83	0.310 (n.s.)	–0.61	–1.97	0.239 (n.s.)	–0.62	–2.60
n	0.712***	–2.57	–3.61	0.108 (n.s.)	–0.15	–1.42	0.048 (n.s.)	–0.09	–1.87
Φ_{hor}	0.020 (n.s.)	0.08	4.30	0.222 (n.s.)	0.35	1.58	0.247 (n.s.)	0.52	2.08

Data are exponents and *P*-values for regressions of log-transformed vertical force ($\mathbf{F}_{vert}$) and power variables ($P_{1.0}$, body mass-specific mechanical power assuming a profile drag coefficient of 1.0; $P_{3.0}$, body mass-specific mechanical power assuming a profile drag coefficient of 3.0) on log-transformed morphological and kinematic variables, including body mass (*m*), flight muscle mass (m_{mus}), wing length (*R*), wing area (*S*), wing loading (p_w), aspect ratio (AR), wingbeat frequency (*n*) and stroke amplitude (Φ_{hor}).

The correlation coefficient (*r*) and *P*-values are derived from the hypothesis that there is no correlation between the two parameters. OLS denotes slopes of regression lines calculated by the ordinary least squares method; RMA denotes slopes of regression lines calculated using the reduced major axis method (*N*=28).

*P<0.05, **P<0.01, ***P<0.001, n.s., P>0.05.

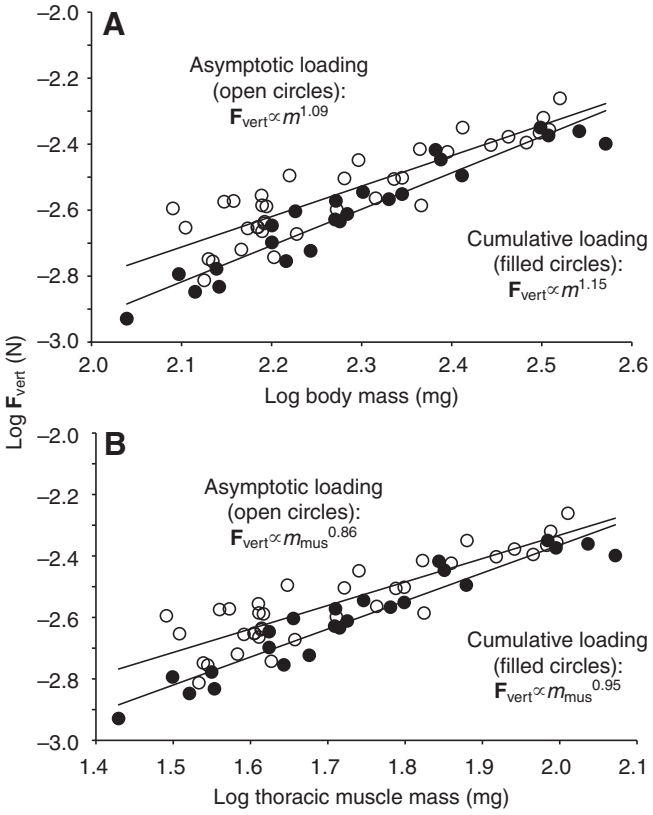

Fig. 1. Comparative allometries of maximum vertical force production derived from two loading methods. (A) Log maximum vertical force ($\mathbf{F}_{vert}$) *versus* log body mass (*m*). Pearson product-moment correlation (asymptotic loading): r=0.883, d.f.=35, r^2=0.78, P<0.0001, RMA regression (asymptotic loading): log$\mathbf{F}_{vert}$=1.09log*m*–4.93. Pearson product-moment correlation (cumulative loading): r=0.955, d.f.=22, r^2=0.99, P<0.0001, RMA regression (cumulative loading): log$\mathbf{F}_{vert}$=1.15log*m*–5.253. The slopes of these two regressions are significantly different (*t*-test: d.f.=1,57, t=25.9, P<0.0001). (B) Log maximum vertical force *versus* log thoracic muscle mass (m_{mus}). Pearson product-moment correlation (asymptotic loading): r=0.883, d.f.=35, r^2=0.78, P<0.0001, RMA regression (asymptotic loading): log$\mathbf{F}_{vert}$=0.86logm_{mus}–4.03. Pearson product-moment correlation (cumulative loading): r=0.955, d.f.=22, r^2=0.99, P<0.0001, RMA regression (cumulative loading): log$\mathbf{F}_{vert}$=0.95logm_{mus}–4.26. The slopes of these two regressions are significantly different (*t*-test: d.f.=1,57, t=16.2, P<0.0001).

based on an average wingbeat frequency of about 181 Hz (range: 155–205 Hz). The average height from the chamber floor attained in such lifting bouts was 13.4 cm (range: 7.9–20.3 cm), which corresponded to approximately 12.8 wing lengths. Lift coefficients for bumblebees in sustained hover at maximum load averaged 2.00 (range: 1.58–2.78), the horizontal projection of stroke amplitude (Φ_{hor}) averaged 144 deg. (range: 131–200 deg.), and Reynolds number (*Re*) averaged 2186 (range: 1608–3004). Although horizontally projected stroke amplitude was independent of body mass [OLS: logΦ_{hor}=2.18–0.01log*m*, P=0.801 (n.s.), RMA: logΦ_{hor}=2.70–0.24log*m*, P=0.652 (n.s.)], wingbeat frequency showed a negative allometry with body mass (log*n*=2.71–0.20log*m*, P<0.0001, RMA: log*n*=2.86–0.27log*m*, P<0.0001). Estimated body weight-specific induced power exhibited positive allometry (Fig. 2), as did estimated body weight-specific profile power when using a drag coefficient of 1.0 (Fig. 3) and body weight-specific mechanical power output for either assumed value of the profile drag coefficient (Fig. 4A). Estimated flight muscle weight-specific mechanical power output showed no relationship with flight muscle mass for either assumed value of the profile drag coefficient (Fig. 4B).

Maximum body mass-specific vertical force decreased significantly (26.3%) after removal of the hindwings and concomitant reduction in total wing area by about one-third and an increase in the non-dimensional radius for the second moment of wing area (N=14; see Table 4). Stroke amplitude under maximum loading differed significantly between controls and experimental treatments (see Table 4). Interestingly, the maximum sustained weight divided by wing area (i.e. $\mathbf{F}_{vert}/S$) was unchanged between control and treatment (44.6±6.0 N m^{-2} and 47.2±7.3 N m^{-2}, respectively; paired *t*-test: t=1.49, d.f.=1,13, P=0.16), although maximum sustained weight divided by the second moment of wing area ($\mathbf{F}_{vert}/S_2$) did change (paired *t*-test: t=3.44, d.f.=1,13, P=0.004). The constancy of effective wing loading during maximum lifting suggests that, in spite of substantial wing reduction, aerodynamic limits to performance relative to sustaining wing area are equivalently reached under the two conditions.

DISCUSSION

Measuring maximum vertical forces

Cumulative application of loads underestimated maximum vertical forces sustained by hovering bumblebees relative to asymptotic load application, and yielded a positive allometry for force production

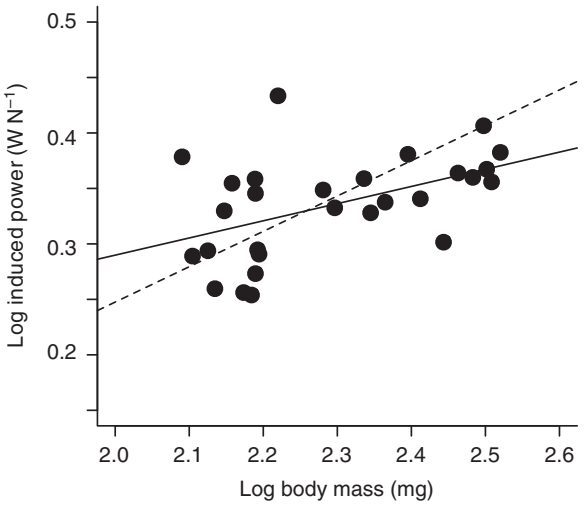

Fig. 2. Allometry of body weight-specific induced power (P_i). Linear regressions as follows – OLS (solid line): logP_i=–0.02+0.15log$m$, P<0.01; RMA (dashed line): logP_i=–0.39+0.32log$m$, P<0.0001. RMA regression is included since individual body mass is variable through time and our one-time measurement is a subsample of this variation.

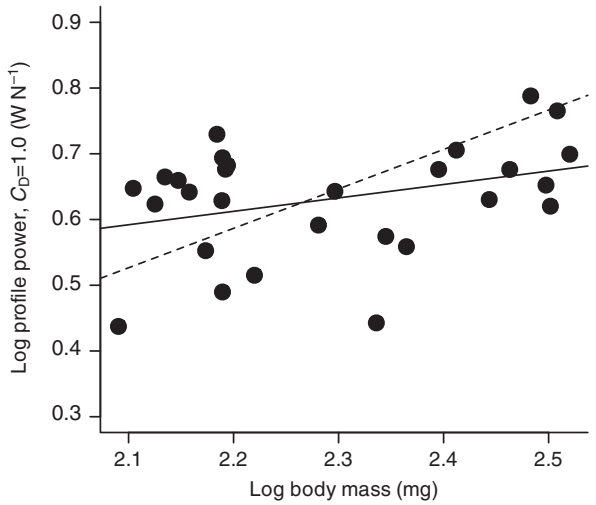

Fig. 3. Allometry of body weight-specific profile power for a profile drag coefficient (C_D) of 1.0. Linear regressions as follows – OLS (solid line): log$P_{1.0}$=0.16+0.20log$m$, P<0.01; RMA (dashed line): log$P_{1.0}$=–0.73+0.60log$m$, P<0.0001. RMA regression is included since individual body mass is variable through time and our one-time measurement is a subsample of this variation.

relative to the absolutely higher but more negatively allometric values obtained through asymptotic loading. Methodological constraints associated with cumulative loading have been discussed elsewhere (Dudley, 2000); paramount among these is the conflation of transient takeoff accelerations (and the ground effect) with sustained hovering at maximum load. Secondarily, possible fatigue or behavioral reluctance to fly following repeated loading may compromise maximum performance. By contrast, asymptotic loading enables quantitative analysis of the effects of repeated trials on estimates of lifting ability; in orchid bees, maximum performance exhibits a statistically significant decline only after 10 or more lifting bouts (see Dillon and Dudley, 2004). Both asymptotic and cumulative methods potentially involve attachment of loads some distance from the center of mass, introducing a pitching moment that may compromise lifting performance *via* adverse increases in body orientation. We note, however, that mass attachment for Hymenoptera using the asymptotic method is at the petiole, a point approximately coincident with the center of body mass (see Ellington, 1984b; Dudley and Ellington, 1990). By contrast, the method of cumulative attachment applies added mass to the ventral surface of the abdomen at points more distant from the center of mass. The associated increase in pitching moment may be partly responsible for the associated underestimate of maximum vertical force production by bumblebees, although it is important to note that Marden did not find a significant effect of load location for dragonflies lifting cumulatively attached weights (Marden, 1987). Further assessment of the role of pitching moments decoupled from overall mass increase is clearly called for in Hymenoptera, particularly given the substantial posterior loading that accompanies nectar feeding in many taxa.

Asymptotic loading also provides increased experimental resolution of maximum forces in that, by altering sizes and numbers of beads on the lifted string, the maximum load can be much more closely estimated than in the cumulative method, in which weights are attached at 20% increments of body mass (Marden, 1987). In sum, these considerations and the present empirical results indicate that, for bumblebees, the cumulative load-lifting method significantly underestimates both maximum values and the allometry of lifting performance. We found asymptotic testing to be preferable for estimating maximum forces and concomitant allometries, and also for the determination of wing and body kinematics that are not well characterized when estimating maximum load with the cumulative technique.

Table 4. Comparison of morphological, kinematic and maximum relative force variables before and after hindwing removal (N=14)

Variable	Hindwings present	Hindwings absent	t-statistic	P-value
S (mm^2)	81.8±18.5	57.4±12.8	14.87	<0.0001
$\hat{r}_2(S)$	0.56±0.01	0.62±0.01	16.23	<0.0001
$\hat{r}_3(S)$	0.60±0.01	0.65±0.01	16.64	<0.0001
p_w (N m^{-2})	29.4±4.1	41.9±5.5	24.0	<0.0001
n (Hz)	177.7±15.6	146.9±25.6	3.08	<0.01
Φ_{hor} (deg.)	141.6±6.6	140.9±7.0	0.40	0.698
$\mathbf{F}_{vert}/m\mathbf{g}$	1.52±0.16	1.12±0.12	8.03	<0.0001

Values are means±s.d. for wing area (S), non-dimensional radius for the second moment of wing area [($\hat{r}_2(S)$)], non-dimensional radius for the third moment of wing area [$\hat{r}_3(S)$], wing loading (p_w), wingbeat frequency (n), horizontally projected stroke amplitude (Φ_{hor}) and body weight-specific vertical force ($\mathbf{F}_{vert}/m\mathbf{g}$).

Allometries of flight performance

Maximum vertical forces generated by bumblebees increased isometrically with respect to body mass, but exhibited a relative decline with respect to thoracic muscle mass (Table 3, Fig. 1). These intraspecific results mirror results of an interspecific comparison of load lifting by orchid bees (Dillon and Dudley, 2004), for which maximum forces significantly declined relative to thoracic muscle mass raised to the power 0.95. Maximum relative forces produced by bumblebees (i.e. $\mathbf{F}_{vert}/m\mathbf{g}$=1.5) were substantially less than values typical of orchid bees (1.8–2.1), consistent with the much higher relative thoracic muscle masses characterizing the latter group (see Dillon and Dudley, 2004). Within *B. impatiens*, thoracic muscle mass scaled allometrically with body mass to the 1.21 power (Table 1), but maximum lifting performance nonetheless exhibited an isometric

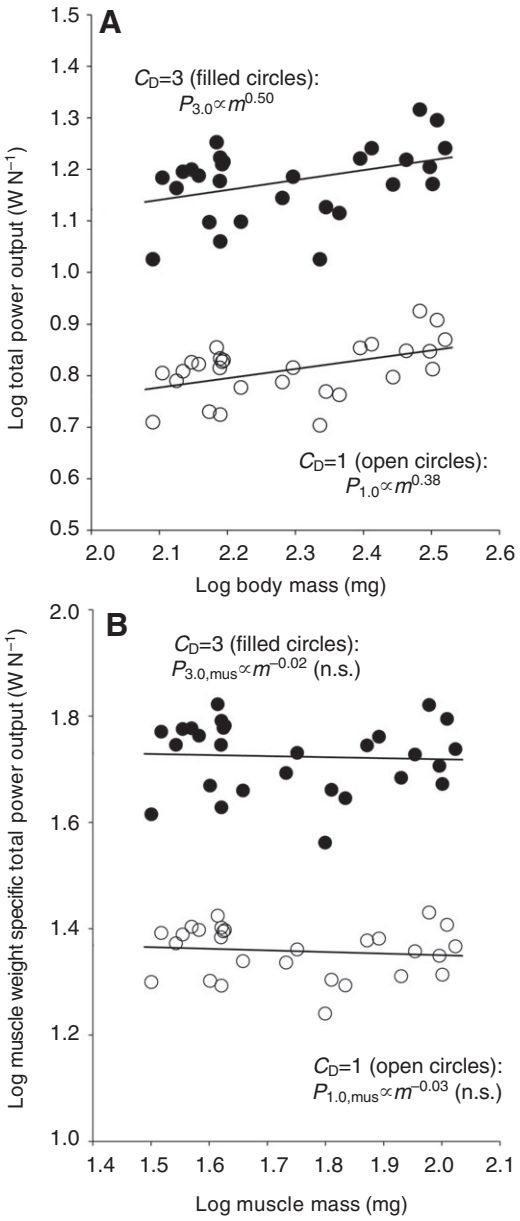

Fig. 4. Allometry of power output in maximum load lifting. (A) Log-transformed body weight-specific mechanical power output for profile drag coefficients of 1.0 and 3.0 ($P_{1.0}$ and $P_{3.0}$, respectively) *versus* log-transformed body mass. Pearson product-moment correlation ($P_{1.0}$): r=0.48, d.f.=26, P<0.01, OLS regression: log$P_{1.0}$=0.399+0.180log$m$, RMA regression: log$P_{1.0}$=–0.043+0.376log$m$, P<0.0001. Pearson product-moment correlation ($P_{3.0}$): r=0.39, d.f.=26, P<0.05, OLS regression: log$P_{3.0}$=0.736+0.192log$m$, RMA regression: log$P_{3.0}$=0.050+0.496log$m$, P<0.0001. (B) Log-transformed flight muscle weight-specific mechanical power output for profile drag coefficients of 1.0 and 3.0 ($P_{1.0,mus}$ and $P_{3.0,mus}$, respectively) *versus* log-transformed flight muscle mass. Pearson product-moment correlation ($P_{1.0,mus}$): r=0.11, d.f.=26, P=0.57 (n.s.), OLS regression: log$P_{1.0,mus}$=1.411–0.030logm_{mus}, RMA regression: log$P_{1.0,mus}$=1.828–0.273logm_{mus}, Pearson product-moment correlation ($P_{3.0,mus}$): r=0.05, d.f.=26, P=0.79 (n.s.), OLS regression: log$P_{3.0,mus}$=1.758–0.020logm_{mus}, RMA regression: log$P_{3.0,mus}$=2.37–0.376logm_{mus}.

relationship with respect to overall size. In contrast to the bumblebees studied here, larger carpenter bees (*Xylocopa varipunctata*) exhibit a negative allometry of thoracic muscle mass, and are correspondingly much less capable of flying in hypodense air relative to their smaller conspecifics (Roberts et al., 2004). Although bumblebees and carpenter bees exhibit opposite allometric trends in thoracic muscle mass, larger individuals of both taxa exhibit a relative reduction in the ability to hover under mechanically limiting conditions. Overall, the combined results of Roberts and colleagues (Roberts et al., 2004), Dillon and Dudley (Dillon and Dudley, 2004), and the present study demonstrate that flight performance in bees is progressively compromised at greater body masses.

Limits to hymenopteran flight performance

As in the studies of Dillon and Dudley (Dillon and Dudley, 2004) and Roberts and colleagues (Roberts et al., 2004), we found here that maximum hovering performance was associated with an upper bound to wing stroke amplitude (~145 deg. for bumblebees and ~140 deg. for carpenter bees and orchid bees). Within bumblebees and carpenter bees, wingbeat frequency at peak performance was also independent of size, raising the possibility of intrinsic kinematic limits on the capacity to augment force production *via* increases in wing translational velocity. Such limits to whole-animal force production are potentially coincident with maximum power produced by the thoracic flight muscle, although other behavioral contexts (e.g. fast forward flight) may associate with yet higher levels of power output albeit at lower stroke amplitudes (see Dudley, 2000). Estimated body weight-specific induced and total mechanical power in maximum lifting exhibited a positive intraspecific allometry with respect to body mass (Fig. 2, Fig. 4A). Given that we do not know the detailed kinematics and associated unsteady drag forces on flapping bumblebee wings, our estimates of profile power should be viewed as approximate, although significant allometric variation in associated profile drag coefficients and in total power estimates is unlikely given the absence of such a trend in the mean lift coefficient (see Table 1). Maximum power output of carpenter bees hovering in hypodense air also showed a generally positive allometry with respect to thoracic muscle mass (Roberts et al., 2004); performance of larger individuals was, however, compromised because of a relatively lower thoracic muscle mass, as mentioned previously. As in Roberts et al. (Roberts et al., 2004), the use here of a bracketing range of profile drag coefficients to estimate the allometry of total power yields results comparable to the allometry of induced power alone. For a profile drag coefficient of 1.0, induced and profile power estimates are of comparable magnitude (Figs 2, 3), and this drag coefficient also corresponds approximately in lift polars to the maximum lift coefficients of rotating bumblebee wing planforms (Usherwood and Ellington, 2002). We accordingly view the associated estimate of total power as more appropriate.

Removal of hindwings from bumblebees resulted in a decline in maximum vertical force production concomitant with the reduction in total wing area, rendering the effective wing loading constant during maximum lifting. By contrast, maximum force expressed relative to the second moment of wing area decreased with the experimental treatment. Cartar found a decrease in wingbeat frequency with a reduction in wing area (Cartar, 1992), and although we found no systematic changes in the horizontal projection of stroke amplitude following hindwing removal (Table 4), wingbeat frequency did decline, suggesting impairment of wing activation. Passive rotational properties of the wing during pronation and supination may have been particularly influenced by hindwing removal. Also, sensory innervation on the hindwing may well influence flight control. A variety of mechanisms thus may underlie the inability of bumblebees to compensate fully to give normal levels of force production following hindwing removal. In aggregate, these results suggest that,

in spite of the much more proximal positioning of hindwing surface area relative to the forewing, it plays an important role in flight. The relevance of hindwing ablation to interpreting natural patterns of trailing edge losses in bumblebees is unclear, however, as the leading edge of the hindwing and associated mass remain mechanically coupled to the forewing under such conditions.

Maximum upwards acceleration potentially influences the outcome of diverse flight behaviors in the context of both natural and sexual selection. It would be naive to assume, however, that the vertical dimension is the sole or necessarily dominant feature of biomechanical relevance for volant taxa. Takeoff in many insects, for example, occurs at various angles relative to gravity and to the vegetational substrate. Many flight maneuvers derive from combined translations along and rotations about multiple orthogonal body axes. It would be of particular interest to determine coupling among maxima in both translational and rotational accelerations, as well as concurrent limits to power production. It is clear that relative thoracic muscle mass, limits on wingbeat kinematics and possibly phylogenetic constraints all interact to influence maximum flight performance of insects. We have focused here on intraspecific variation in load lifting by bumblebees to remove potentially confounding phylogenetic effects of non-random species associations. Interspecific analysis of the limits to hovering performance, using the method of either asymptotic loading or hypodense gas mixtures, would provide a valuable comparison to existing literature so as to broaden our understanding of the allometry of force and power production among flying animals.

APPENDIX

Methods for lift and power calculations

Aerodynamic equations used for lift and power estimates during hovering were those of Ellington (Ellington, 1984d), with the exception that the effective body mass incorporated the additional external load sustained during lifting (body weight-specific results for force and power production, however, refer to the anatomical body mass). Mean Reynolds numbers for wings were calculated using the mean wing chord and the mean wingtip velocity, assuming simple harmonic motion. Mean lift coefficients were calculated such that vertical force production averaged over the wingbeat period equalled effective body weight; the downstroke and upstroke were assumed to contribute equally to vertical force production. Mechanical power requirements of flight were estimated by evaluating the individual components of profile and induced power. Profile power represents energetic expenditure to overcome profile drag forces on the wings, while induced power corresponds to the power necessary to generate sufficient downwards momentum to the surrounding air so as to offset the body weight. Profile power was calculated assuming simple harmonic motion of the wings in the stroke plane and an assumed value for the profile drag coefficient, as mentioned previously. Induced power was calculated using a modified version of the Rankine–Froude momentum estimate, assuming the actuator disc area to be the horizontally projected stroke amplitude. Two independent correction factors reflecting non-uniform wing circulation and wake periodicity were added linearly to this estimate. Inertial power requirements through the wingbeat were assumed to be zero given the likelihood of elastic energy within the hymenopteran thorax; in this case of perfect elastic energy storage, mechanical power expenditure then equals the sum of profile and induced powers. For data see Table S1 in supplementary material.

LIST OF SYMBOLS AND ABBREVIATIONS

AR	wing aspect ratio
C_D	drag coefficient
C_L	lift coefficient
$\mathbf{F}_{vert}$	vertical force
$\mathbf{F}_{vert}/m\boldsymbol{g}$	body weight-specific vertical force
$\boldsymbol{g}$	gravitational acceleration
m	body mass
m_{mus}	thoracic muscle mass
m_{th}	thoracic mass
n	wingbeat frequency
p_w	wing loading
P_i	body weight-specific induced power
P_{mus}	thoracic muscle weight-specific power output
$P_{1.0}$	body weight-specific power output using a profile drag coefficient of 1.0
$P_{1.0,mus}$	thoracic muscle weight-specific power output using a profile drag coefficient of 1.0
$P_{3.0}$	body weight-specific power output using a profile drag coefficient of 3.0
$P_{3.0,mus}$	thoracic muscle weight-specific power output using a profile drag coefficient of 3.0
$\hat{r}_2(S)$	non-dimensional radius for the second moment of wing area
$\hat{r}_3(S)$	non-dimensional radius for the third moment of wing area
R	wing length
Re	Reynolds number
S	wing surface area
S_2	second moment of wing area
Φ_{hor}	horizontal projection of stroke amplitude

ACKNOWLEDGEMENTS

We thank Koppert Biological for assistance with bumblebee colonies, and the NSF (DBI-0610265 and DEB-0543556) for research support. Michael Dillon and multiple anonymous reviewers provided invaluable comments on the manuscript.

REFERENCES

Altshuler, D. L. and Dudley, R. (2003). Kinematics of hovering hummingbird flight along simulated and natural elevational gradients. *J. Exp. Biol.* **206**, 3139-3147.
Cartar, R. V. (1992). Morphological senescence and longevity: an experiment relating wing wear and life span in foraging wild bumble bees. *J. Anim. Ecol.* **61**, 225-231.
Chai, P., Chen, J. S. C. and Dudley, R. (1997). Transient hovering performance of hummingbirds under conditions of maximal loading. *J. Exp. Biol.* **200**, 921-929.
Dillon, M. E. and Dudley, R. (2004). Allometry of maximum vertical force production during hovering flight of neotropical orchid bees (Apidae: Euglossini). *J. Exp. Biol.* **27**, 417-425.
Dudley, R. (1995). Extraordinary flight performance of orchid bees (Apidae: Euglossini) hovering in heliox (80% He/20% O_2). *J. Exp. Biol.* **198**, 1065-1070.
Dudley, R. (2000). *The Biomechanics of Insect Flight: Form, Function, Evolution.* Princeton, New Jersey: Princeton University Press.
Dudley, R. and Ellington, C. P. (1990). Mechanics of forward flight in bumblebees. I. Kinematics and morphology. *J. Exp. Biol.* **148**, 19-52.
Ellington, C. P. (1984a). The aerodynamics of hovering insect flight. I. The quasi-steady analysis. *Phil. Trans. R. Soc. Lond. B* **305**, 1-15.
Ellington, C. P. (1984b). The aerodynamics of hovering insect flight. II. Morphological parameters. *Phil. Trans. R. Soc. Lond. B* **305**, 17-40.
Ellington, C. P. (1984c). The aerodynamics of hovering insect flight. III. Kinematics. *Phil. Trans. R. Soc. Lond. B* **305**, 41-78.
Ellington, C. P. (1984d). The aerodynamics of hovering insect flight. VI. Lift and power requirements. *Phil. Trans. R. Soc. Lond. B* **305**, 145-181.
Ellington, C. P. (1991). Limitations on animal flight performance. *J. Exp. Biol.* **160**, 71-91.
Hedenström, A., Ellington, C. P. and Wolf, T. J. (2001). Wing wear, aerodynamics and flight energetics in bumblebees (*Bombus terrestris*): an experimental study. *Func. Ecol.* **15**, 417-422.
Heinrich, B. (1970). *Bumblebee Economics*. Cambridge, MA: Harvard University Press.
Marden, J. H. (1987). Maximum lift production during takeoff in flying animals. *J. Exp. Biol.* **130**, 235-258.
Marden, J. H. (1990). Maximum load-lifting and induced power output of Harris' Hawks are general functions of flight muscle mass. *J. Exp. Biol.* **149**, 511-514.
Roberts, S. P., Harrison, J. F. and Dudley, R. (2004). Allometry of kinematics and energetics in carpenter bees (*Xylocopa varipunctata*) hovering in variable-density gases. *J. Exp. Biol.* **207**, 993-1004.
Sane, S. and Dickinson, M. H. (2001). The control of flight force by a flapping wing: lift and drag production. *J. Exp. Biol.* **204**, 1565-1576.
Usherwood, J. R. and Ellington, C. P. (2001). The aerodynamics of revolving wings. II. Propeller force coefficients from mayfly to quail. *J. Exp. Biol.* **205**, 2607-2626.

Table S1. Morphological, kinematic and load-lifting data for individual bees

Method tested	Date	Body mass (mg)	Mass of abdomen (mg)	Mass of thorax (mg)	Mass of wing pair (mg)	Total lifted (mg)	Wing area (mm^2)	Wing length (mm)	$\hat{r}_2(S)$	Aspect ratio	p_w	Frequency (Hz)	Stroke amplitude (deg.)	$\mathbf{F}_{vert}$ (N)	$\mathbf{F}_{vert}/mg$
Asymptotic	2-Nov-06	232.35	110.92	80.27	0.48	264.88	82.27	12.25	0.56	7.30	27.71	n/a	n/a	0.00260	1.14
Asymptotic	2-Nov-06	132.63	59.53	47.54	0.19	147.60	n/a	n/a	n/a	n/a	n/a	n/a	n/a	0.00145	1.11
Asymptotic	2-Nov-06	169.00	73.90	62.97	0.20	217.05	64.38	10.61	0.56	6.99	25.75	n/a	n/a	0.00213	1.28
Asymptotic	3-Nov-06	146.68	65.01	52.40	0.50	194.73	55.41	9.97	0.55	7.17	25.97	n/a	n/a	0.00191	1.33
Asymptotic	6-Nov-06	159.46	70.80	55.88	0.22	184.54	62.89	11.25	0.57	8.05	24.88	n/a	134.77	0.00181	1.16
Asymptotic	6-Nov-06	206.77	96.35	70.73	0.40	278.44	76.62	11.15	0.55	6.49	26.47	n/a	148.49	0.00273	1.35
Asymptotic	6-Nov-06	134.87	57.09	47.61	0.16	182.23	56.53	9.78	0.55	6.77	23.41	n/a	143.44	0.00179	1.35
Asymptotic	6-Nov-06	155.54	74.25	51.15	0.15	233.75	55.32	9.34	0.54	6.31	27.58	n/a	154.88	0.00229	1.50
Asymptotic	8-Nov-06	154.68	68.70	55.41	0.32	221.25	62.17	10.65	0.56	7.30	24.41	190.00	134.44	0.00217	1.43
Asymptotic	22-Nov-06	140.37	57.75	51.35	0.25	271.87	59.16	9.72	0.57	6.38	23.28	200.00	148.50	0.00266	1.94
Asymptotic	22-Nov-06	154.68	75.74	49.70	0.24	265.04	57.21	9.70	0.57	6.58	26.52	185.00	141.51	0.00260	1.71
Asymptotic	22-Nov-06	143.81	62.94	46.04	0.28	273.27	57.93	10.11	0.56	7.06	24.35	205.00	138.53	0.00268	1.90
Asymptotic	22-Nov-06	123.13	50.05	45.03	0.24	259.44	51.31	9.38	0.56	6.85	23.54	190.00	141.02	0.00254	2.11
Asymptotic	29-Nov-06	165.91	68.72	62.76	0.28	326.44	66.55	10.15	0.55	6.19	24.46	190.00	136.87	0.00320	1.97
Asymptotic	29-Nov-06	149.07	74.95	44.33	0.20	225.71	49.99	9.82	0.59	7.72	29.26	190.00	141.67	0.00221	1.51
Asymptotic	29-Nov-06	155.70	68.70	49.90	0.31	236.32	65.67	10.48	0.56	6.69	23.26	190.00	135.32	0.00232	1.52
Asymptotic	29-Nov-06	216.75	113.72	63.35	0.28	318.60	72.27	11.14	0.56	6.86	29.42	155.00	139.61	0.00312	1.47
Asymptotic	29-Nov-06	197.92	76.59	79.86	0.46	363.50	83.29	11.93	0.56	6.83	23.31	160.00	146.75	0.00356	1.84
Asymptotic	29-Nov-06	231.52	106.35	82.34	0.44	392.50	81.85	12.01	0.57	7.04	27.75	160.00	141.03	0.00385	1.70
Asymptotic	29-Nov-06	133.40	66.53	40.71	0.20	157.08	49.91	9.07	0.55	6.59	26.22	200.00	136.42	0.00154	1.18
Asymptotic	1-Dec-06	152.81	74.27	49.70	0.20	227.46	59.68	10.07	0.57	6.80	25.12	180.00	157.80	0.00223	1.49
Asymptotic	1-Dec-06	154.47	67.57	55.35	0.28	283.93	63.13	10.36	0.55	6.79	24.01	190.00	142.23	0.00278	1.84
Asymptotic	1-Dec-06	248.47	124.30	79.04	0.37	384.78	84.26	11.69	0.55	6.48	28.93	170.00	146.79	0.00377	1.55
Asymptotic	18-Jan-07	127.18	58.66	42.79	0.20	226.83	58.06	9.15	0.59	5.77	21.49	200.00	147.95	0.00222	1.78
Asymptotic	18-Jan-07	304.05	158.39	89.51	0.49	410.77	88.83	11.91	0.55	6.38	33.58	180.00	148.93	0.00403	1.35
Asymptotic	23-Jan-07	314.41	173.97	90.15	0.37	439.97	84.36	11.93	0.55	6.74	36.56	180.00	139.46	0.00431	1.40
Asymptotic	23-Jan-07	190.91	90.81	63.90	0.25	319.81	68.94	10.75	0.57	6.71	27.17	190.00	134.51	0.00313	1.68
Asymptotic	24-Jan-07	317.47	162.92	99.26	0.48	488.50	102.66	13.09	0.56	6.67	30.34	155.00	139.68	0.00479	1.54
Asymptotic	24-Jan-07	290.38	140.47	93.90	0.46	427.81	96.32	12.33	0.55	6.31	29.57	155.00	151.21	0.00419	1.47
Asymptotic	30-Jan-07	331.24	163.00	107.05	0.63	559.27	104.02	13.41	0.56	6.91	31.24	170.00	137.56	0.00548	1.69
Asymptotic	12-Feb-07	221.28	98.00	71.07	0.38	321.27	65.42	11.12	0.57	7.56	33.18	190.00	130.83	0.00315	1.45
Asymptotic	12-Feb-07	156.40	71.42	54.70	0.23	263.12	61.22	10.45	0.58	7.14	25.06	200.00	137.40	0.00258	1.68
Asymptotic	12-Feb-07	322.32	150.66	110.71	0.63	449.34	110.14	13.18	0.55	6.31	28.71	165.00	138.29	0.00440	1.39
Asymptotic	13-Feb-07	258.29	123.43	84.93	0.50	456.03	86.13	12.08	0.57	6.78	29.42	170.00	152.62	0.00447	1.77
Asymptotic	13-Feb-07	136.35	58.67	44.69	0.27	179.21	55.98	9.60	0.57	6.59	23.89	190.00	140.82	0.00176	1.31
Asymptotic	13-Feb-07	277.62	132.44	91.60	0.57	403.85	81.92	12.41	0.58	7.53	33.25	165.00	141.04	0.00396	1.45

Method tested	Date	Body mass (mg)	Mass of abdomen (mg)	Mass of thorax (mg)	Mass of wing pair (mg)	Mass lifted (mg)	Non-lifted mass (mg)	F_{vert} (N)	F_{vert}/mg
Cumulative	9-Dec-06	158.60	70.12	53.72	0.29	189.6	219.7	0.00201	1.29
Cumulative	11-Dec-06	213.90	109.83	69.25	0.38	256	297.5	0.00271	1.29
Cumulative	11-Dec-06	109.44	49.33	37.14	0.23	109.44	130.94	0.00118	1.10
Cumulative	11-Dec-06	188.68	51.92	99.36	0.39	221.78	252.18	0.00232	1.26
Cumulative	11-Dec-06	257.87	75.61	132.91	0.44	305.97	347.17	0.00320	1.27
Cumulative	11-Dec-06	137.66	92.20	51.52	0.25	20.75	44.95	0.00167	1.24
Cumulative	11-Dec-06	192.32	88.75	70.63	0.39	42.99	72.29	0.00245	1.30
Cumulative	11-Dec-06	158.62	69.89	58.55	0.29	59.29	84.79	0.00226	1.45
Cumulative	13-Dec-06	175.10	87.90	53.08	0.25	175.1	210.9	0.00189	1.10
Cumulative	13-Dec-06	168.40	87.82	56.40	0.30	237.4	271.2	0.00249	1.51
Cumulative	13-Dec-06	164.48	85.85	50.30	0.28	164.48	194.78	0.00176	1.09
Cumulative	31-Jan-07	200.20	94.01	64.75	0.28	77.88	104.28	0.00285	1.45
Cumulative	31-Jan-07	186.42	90.74	50.90	0.35	37.25	70.95	0.00235	1.29
Cumulative	31-Jan-07	321.66	165.46	98.37	0.43	94.23	126.63	0.00423	1.34
Cumulative	31-Jan-07	241.02	61.12	104.78	0.50	138.7	160.85	0.00382	1.62
Cumulative	31-Jan-07	244.29	116.76	79.54	0.42	97.62	144.72	0.00358	1.49
Cumulative	31-Jan-07	348.02	186.02	99.39	0.53	63.63	130.83	0.00436	1.28
Cumulative	31-Jan-07	315.18	142.59	109.68	0.66	115.56	167.66	0.00447	1.45
Cumulative	31-Jan-07	221.26	115.65	62.93	0.26	44.66	86.86	0.00281	1.30
Cumulative	31-Jan-07	372.33	196.69	107.53	0.62	0.62	70.82	0.00399	1.09
Cumulative	6-Feb-07	138.61	58.01	45.84	0.23	0.23	23.33	0.00147	1.08
Cumulative	6-Feb-07	130.33	56.87	44.40	0.21	0.21	29.51	0.00142	1.11
Cumulative	6-Feb-07	125.02	58.35	43.48	0.27	24.77	53.87	0.00161	1.31
Cumulative	6-Feb-07	186.79	87.00	64.31	0.28	71.38	102.58	0.00268	1.46

Measurements on the first eight bees used in asymptotic load-liftiing did not include wingbeat frequencies, and associated data were used only in force and not power allometries.